Journal of Sustainable Metallurgy
https://doi.org/10.1007/s40831-026-01461-8

RESEARCH ARTICLE

Fayalitic Minerals and Slags (Part II): Physical Properties and Metal Distribution Simulation

Joao Weiss[1] · **Daniel Munchen**[1] · **Hugo Lucas**[1] · **Bernd Friedrich**[1]

Received: 26 September 2025 / Accepted: 10 February 2026

Abstract

The interaction between fayalitic slags and nonferrous metals during smelting presents a multifaceted challenge that necessitates comprehensive investigation to enhance metallurgical processes toward the recovery of valuable metals. This study builds on the literature review of the composition and mineralogy of fayalitic slags (Part I), examining the effect of these composition on thermodynamic and physical properties, which were generated through thermochemical simulations using available databases and known studies. The findings and models created have shown that small changes in composition have significant effects on properties. For each property studied an equation was derived from the model to summarize and simplify complex calculations. Differences between predicted values and experimental results were also commented. Melting temperature, for example, increases mainly with the CaO content increase, reaching up to 1600 °C. On the other hand, SiO_2 content increase plays a more significant role in the increase of viscosity, where values of up to 3 Pa·s were observed. Meanwhile, the FeO content increase has shown significant effect on density, up to 3.4 g·cm^{-3}. The addition of secondary compounds (fluxes) such as Al_2O_3, MgO, and Fe_2O_3 have also influenced the melting temperature, viscosity, and density of fayalitic slags, with 9 mass% Al_2O_3 notably expanding the low-viscosity area between 0.1 and 1 Pa·s and altering density ranges, while Fe_2O_3 effectively reduces viscosity more than CaO. The combination of these compounds further modify the properties, enhancing the potential for targeted mineral enrichment in fayalitic slags. The study demonstrates how slag composition adjustments can lower melting temperatures and viscosity, while reducing the heat input and energy needs. Regression models enable efficient fayalitic slags designs aligned with sustainable goals, thereby reducing overall carbon footprint, facilitating slag reprocessing for metal extraction, minimizing waste, and environmental impact.

The contributing editor for this article was Hiromichi Takebe.

✉ Joao Weiss
jweiss@ime-aachen.de

[1] IME Process Metallurgy and Metal Recycling, Institute of RWTH Aachen University, Intzestraße 3, 52056 Aachen, Germany

Published online: 16 March 2026

Graphical Abstract

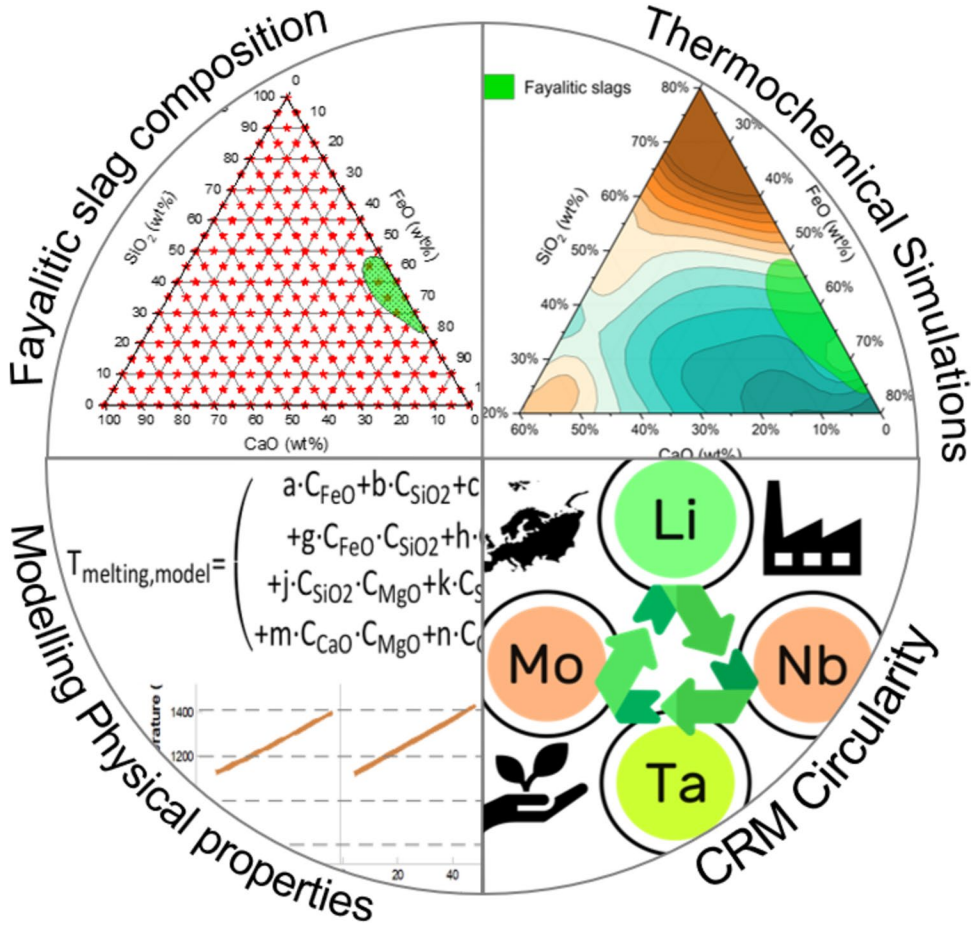

Keywords Fayalitic slags · Slag design · Thermochemical simulations · Physical properties

Introduction

Among the various metal reduction operations in the current pyrometallurgical industry, the adoption of fayalitic slag as a versatile constituent has been consolidated due to its unique properties and potential benefits in metallurgical processes, such as a lower melting point and enhanced mobilization of iron. These slags, primarily composed of Fayalite (Fe_2SiO_4), are typically formed during the smelting of iron and nonferrous metals. They have already demonstrated high efficiency and sustainable operations in metal recovery by reducing energy consumption through improved heat retention and transfer. Furthermore, the presence of fayalitic slags in smelting operations can enhance fluidity, which facilitates higher overall recovery rates of valuable metals [1–3].

In addition to their operational advantages, fayalitic slags also offer opportunities for environmental sustainability. In recent years, the reprocessing of such slags has increased, allowing further recycling of lost metals, reuse in smelting operations multiple times, and utilization in the cement industry as aggregate. These practices help mitigate the environmental impacts associated with traditional disposal methods [4, 5]. Incorporating fayalitic slags into the smelting process can reduce the need for virgin materials, thereby minimizing the ecological footprint of metal production. Moreover, the chemical composition of fayalitic slags can be engineered to capture and immobilize harmful or valuable elements, reducing losses and enhancing the overall environmental performance of smelting operations while generating profit and increasing circularity [6].

By altering the properties of fayalitic slags and engineering new minerals, target metals could be recovered. For instance, fayalitic slags exhibit properties that facilitate the formation of a liquid phase at elevated temperatures (> 1200 °C). It has been reported that, with a composition of 71 mass% FeO and

29 mass% SiO_2, the liquidus temperature is approximately 1200 °C [7]. The addition of fluxing agents to the system, such as CaO or Al_2O_3, influences this liquidus temperature. Specifically, when Al_2O_3 is added to the FeO–SiO_2–CaO system, a decrease of 3 K in liquidus temperature is observed for each 1 mass% of Al_2O_3 added [8]. This characteristic is particularly advantageous in nonferrous smelting operations, where the separation of target metals from remaining impurities is crucial.

The interaction between fayalitic slags and various nonferrous metals during the smelting process is a complex phenomenon that requires further investigation. Understanding the thermodynamic and kinetic behaviors of these slags in conjunction with different metallurgical sources can lead to the optimisation of smelting parameters and the development of innovative processing techniques. Research in this area has the potential to yield significant advancements in slag design efficiency, engineering target mineralogical phase enrichment for metal recovery, and improvements in the economic viability of nonferrous smelting operations [9, 10]. Despite the promising attributes of fayalitic slags, challenges remain in their widespread adoption. Variability in slag composition, the need for precise control of smelting conditions, and the integration of these materials into existing processes are some hurdles that must be addressed. Additionally, further research is needed to elucidate the long-term performance and stability of fayalitic slags in various operational scenarios.

In this context, thermodynamic simulations play a crucial role in the pyrometallurgical industry, particularly in the research and development of new slag designs. These simulations enable engineers and researchers to predict phase equilibria, chemical reactions, and thermodynamic properties under varying conditions, all of which are essential for optimizing processes such as smelting and refining metals. By accurately modeling the behavior of slags, researchers can design tailored slag compositions that enhance efficiency, reduce energy consumption, and minimize environmental impacts. Furthermore, thermodynamic tools help in understanding how different variables affect slag performance, ultimately leading to innovations that improve resource recovery and contribute to more sustainable practices within the industry.

The goal of this publication is to determine the thermochemical and physical properties of fayalitic slags through composition simulations utilizing FactSage 8.3™ and other computational tools. Our aim is to analyze the variations in slag behavior under different conditions and evaluate how these changes can enhance the recovery of valuable metals from specific minerals. By offering a thorough assessment of the engineered slags, we intend to demonstrate that customized slag designs can significantly improve metal recovery processes, thus contributing to more efficient and sustainable practices within the pyrometallurgical industry.

Methodology

Initially, the compounds and their corresponding compositional ranges for the simulations were established. Based on the research from Part I [11], FeO, SiO_2, and CaO were identified as the *primary compounds* in fayalitic slags; therefore, these served as the baseline for simulations at each point in the ternary diagram shown in Fig. 1, which represents increments of 5 mass%. In addition to the primary compounds, *secondary compounds*—Fe_2O_3, Al_2O_3, and MgO – were included in the simulation based on reasonable values outlined in Part I, which were, respectively, 10 mass%, 9 mass%, and 3 mass%. These values represent each maximum compound composition of percentile 75 %. When these secondary compounds were incorporated, the composition of the primary compounds was normalized to ensure that the sum of 100 mass% was always achieved. The inclusion of Fe_2O_3 aimed to investigate the influence of iron speciation since much of the literature does not differentiate between Fe^{2+} and Fe^{3+}. Al_2O_3 and MgO were added because these elements, along with CaO, represent three of the most commonly found fluxes in fayalitic slags and are crucial for modulating viscosity, density, basicity, and melting temperature. In total, 1056 compositions were simulated.

Statistical analyses were also conducted using the regression models in Minitab™ 2017 to visualize the main effects of the composition variation of primary and secondary compounds on the properties under investigation. To increase the accuracy of regression equations, only the calculated data from the green

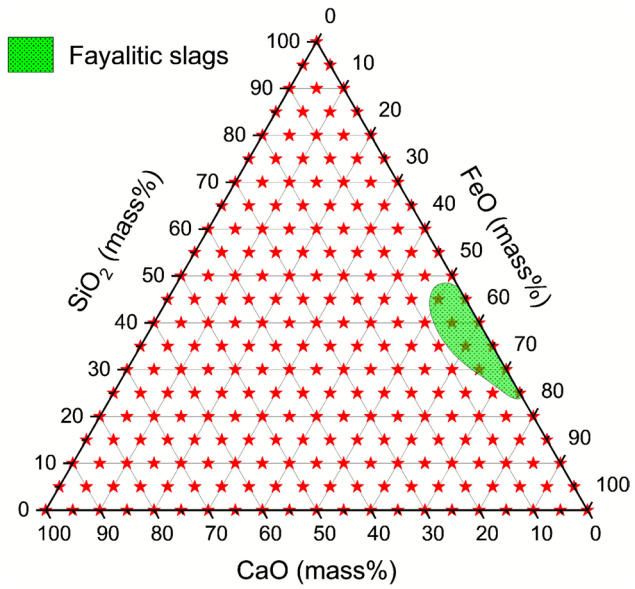

Fig. 1 CaO–FeO–SiO_2 ternary diagram with marked points (in red) corresponding to the compositions used for the baseline simulation. The green area represents the majority composition of industrial fayalitic slags in Part I

area of Fig. 1 were utilized. For the regressions, a Box–Cox transformation (for finding an optimum coefficient as a nonlinear function) and stepwise elimination were utilized to minimize the number of coefficients and maximize the R^2 of the prediction. Consequently, modeled equations for each property were provided as an alternative means of validating of the respective property.

Thermochemical and Physical Properties

The composition determines the liquidus temperature, whereby the slag phase is completely in a liquid state. For this, the *Equilib* module on the start menu of the FactSage™ software was selected, using modeling databases FactPS and FToxid. In the software window, the slag phase was therefore selected as precipitated target phase so the melting temperature of these slags would be calculated. Subsequently, additional simulations were conducted at four fixed temperatures: 25 °C, 1100 °C, 1200 °C, and 1300 °C to assess the other properties.

Enthalpy (H) and Heat capacity (C_p) were obtained for the compositions in the studied range of temperatures. The enthalpy variation (ΔH) was then calculated as the difference between the values at 25 °C and at the studied temperature or the calculated melting temperature.

For estimating the density of the system, the same databases of FactSage™ were utilized to calculate the solid fraction (x_s). Then, the model based on optical basicity from Shu and Chou [12] (see Eqs. 2–7) was utilized to calculate the density of the melt. Finally, the density of the system was calculated through the following expression:

$$\rho = \rho_s \cdot x_s + \rho_l \cdot \left(1 - x_s\right) \tag{1}$$

where ρ is the density of the system in g·cm^{-3}, ρ_s is the density of the solid fraction, x_s is the solid fraction in mass% calculated by FactSage™ and ρ_l is the density of the melt.

$$K = \exp\left[4.662 \cdot \left(\sum_i x_{M_i^{V+}}/\Lambda_{M_i^{V+}} - \sum_j x_{T_j^{n+}}/\Lambda_{T_j^{n+}}\right) - 1.1445\right] \tag{2}$$

$$N_{O^{-\prime}} = \frac{-\left(1 + x_{SiO_2}\right) + \left[\left(1 + x_{SiO_2}\right)^2 - 8 \cdot (4 \cdot K - 1) \cdot x_{SiO_2} \cdot \left(x_{SiO_2} - 1\right)\right]^{1/2}}{(4 \cdot K - 1)} \tag{3}$$

$$\Delta G_{mix} = \frac{N_{O^-}}{2} \cdot RT \cdot \ln K \tag{4}$$

$$V_i = V_0 + \beta \cdot T \tag{5}$$

$$V_{system} = \sum x_i \cdot V_i \cdot \left(1 + \frac{\lambda \cdot \Delta G_{mix}}{R \cdot T}\right) \tag{6}$$

$$\rho = \frac{\sum x_i \cdot M_i}{V_{system}} \tag{7}$$

where $x_{M_i^{V+}}$ and $x_{T_j^{n+}}$ are the molar fractions of network modifying and network forming cations, respectively; $\Lambda_{M_i^{V+}}$ and $\Lambda_{T_j^{n+}}$ are the optical basicity coefficients for the network modifiers and formers (Table 1); x_{SiO_2} is the molar fraction of SiO_2 in the melt; N_{O^-} is the nonbridged oxygen, calculated using the model of Toop and Samis (1962) [14, 15], and K is the equilibrium constant based on the correlation made by Ottonello et al. [16]. λ is a constant defined as 0.025, x_i, M_i, and V_i are the molar fraction, molar mass, and molar volume of each oxide in the system, respectively. Finally, R is the constant of gases and T is the temperature in Kelvin.

The ideal viscosity of the melt was calculated using FactSage™ and subsequently corrected with the Roscoe model [17], which accounts for the presence of solid particles and their influence on liquid viscosity. This solid fraction was determined for all studied points in the ternary diagram, including the secondary compounds and temperatures. The final equation for the slurry viscosity η_s is as follows:

$$\eta_s = \eta_l \cdot (1 - x_s)^{-n} \tag{8}$$

where η_l is the ideal liquid viscosity, x_s is the solid fraction, and n is an empirical parameter obtained from literature and fixed at 2.5 [18].

Distribution Coefficients of Metals Between Phases

The elements dissolved in fayalitic slags (slagging) are directly related to the equilibrium conditions [19, 20].

Table 1 Optical basicity coefficients for the network forming and modifying cations used in Eq. (2) for primary and secondary compounds in density modeling [12, 13]

Oxide	CaO	MgO	Al_2O_3 (IV)	Al_2O_3 (VI)	SiO_2	FeO	Fe_2O_3
Network forming cations	0	0	1	0	1	0	1
Network modifying cations	1	1	0	1	0	1	0

Therefore, the slagging is a function of its equilibrium constant, the process temperature, and the prevalent oxygen partial pressure of the system.

The overall average composition of the slagging in fayalitic slags from Part I was normalized and the minor elements' concentration was simplified by bringing the normalized values to the corresponding closest values of 1500, 1000 or 500 ppm, according to Table 2.

For modeling the distribution coefficients of metals present in this specific fayalitic slag, FactPS, FToxid, and FTlite databases were used, varying the carbon activity between 1×10^{-25} and $1\times10^{+3}$ in logarithm steps. This variation in carbon activity is translated into the system's oxygen partial pressure and utilized to calculate the carbon excess required to achieve the desired metal's activity, as well as its indirect influence on the distribution of metals between the metal, gas, and slag phases.

In a multi-component system, the constant of equilibrium will consider not only the partial pressure of the system, but also the concentration of each element in the metal and in the slag system. From this point, the distribution coefficient slag/metal, which help to identify when an element is immobilized in the slag, was defined according to the following expression [19]:

$$L_{Me}^{slag/metal} = \frac{C_{Me}^{slag}}{C_{Me}^{metal}} \tag{9}$$

where C_{Me}^{slag} and C_{Me}^{metal} correspond to the concentration of metal (Me) in the slag phase and in metal phase, respectively.

To avoid errors where the calculation shows 0 mass% of an element, a mathematical zero equal to 1×10^{-20} was implemented. Besides, it was defined that the minimal and maximal values in logarithmic scale of the calculated distribution coefficients were between 1×10^{-12} and 1×10^{12}. This means that an element is 10 billion times more concentrated in one phase compared to the second one.

Results and Discussion

Melting Temperature

In general, in carbothermic reduction process, iron should be reduced from Hematite (Fe_2O_3) to its metallic form at temperatures close to 700 °C. However, in the presence of silica (SiO_2), the reduction of iron tends to stall in the form of FeO for temperatures below 1300 °C, which then tends to form fayalite with melting point of around 1200 °C. Once fayalite is formed under normal conditions in air atmosphere, it will tend to decompose as the slag cools into a mixture of magnetite (Fe_3O_4) and silica. Generally, due to mineralogical and kinetic complexity, fayalite never fully decomposes at low temperatures (<900 °C), resulting in industrial slags being a mixture of an amorphous matrix with magnetite and fayalite in varying concentrations, along with several other types of minerals that may precipitate [21, 22]. If the concentration of silica decreases, the activity of iron oxide will increase, and its reduction capacity will also rise. High concentrations of FeO in the slag will transform upon cooling into a mixture of metallic iron and magnetite if there is not enough silica present in the system.

Figure 2a shows the simulated melting temperatures for the primary compounds in the ternary composition system. The green area on the right sets where the majority of fayalitic slags composition in Part I [11] were reported. Within this area, the fayalitic slags shows melting temperature in a range from 1100 to 1500 °C. On the other hand,

Figure 2b illustrates the influence of the secondary compounds in fayalitic slags and their combinations. For example, the increase in Fe^{3+} concentration has a positive effect on lowering melting temperature. This also aligns with processing conditions where slags are in direct contact with air, which makes speciation of iron as a combination of Fe^{2+} and Fe^{3+} inevitable and favorable according to thermochemical models. Depending on the compounds' content combinations, a positive effect on decreasing the melting temperature could be achieved, demonstrating that with the secondary compounds addition, the entirety of the green area will present melting temperatures below 1200 °C; this is not only critical for reducing process costs but it also stabilizes iron in the slag phase improving the

Table 2 Minor elements composition used in the slagging distribution modeling

Mass%									
Fe	Si	Ca	Al	Cu	Mg	Zn	S	Pb	O
35.79	15.19	4.85	2.41	1.59	1.50	1.47	0.78	0.56	34.97
ppm									
Co	As	Ni	P	Cr	Mo	Sb	Cd	Nb	Ta
1500	1500	1500	1000	1000	500	500	500	500	500

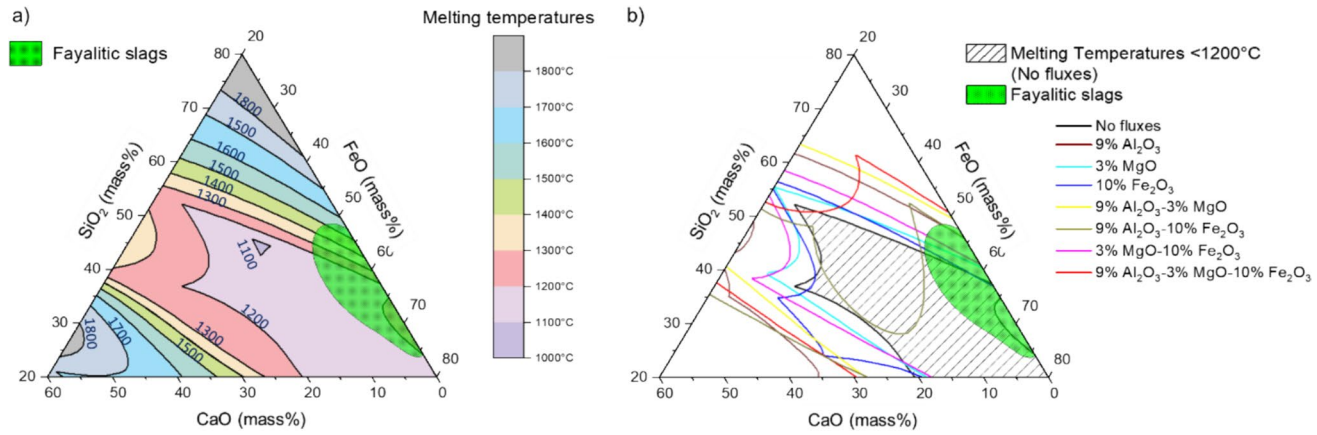

Fig. 2 Melting temperatures: **a** primary compounds CaO–FeO–SiO_2; and **b** primary and secondary compounds (MgO, Fe_2O_3, and Al_2O_3) at 1200 °C. The green area in both graphs represents the majority composition of industrial fayalitic slags in Part I

quality of targeted nonferrous metals, such as Sn, Sb, Co, Cu, Ni, Pb, and precious metals that might be recovered in reduction processes involving the fayalitic slags [23].

In addition, a significant change around 1200 °C of melting temperature is observed by the dark yellow line, which stands for 9 mass% Al_2O_3 and 10 mass% Fe_2O_3. However, maintaining these two contents, but adding 3 mass% of MgO (red line), the area is expanded, comprehending the whole green area of the researched fayalitic slags. Solely with the addition of 9 mass% Al_2O_3, the area increases following the brown line.

It must be noted that such analysis is only a prediction by a thermochemical software, and therefore, differences between the predicted values and experimental results have been already documented.

For slag systems containing 15 mass% or a combined CaO + MgO content of 55 mass%, the thermodynamic database in the software is expected to predict melting temperatures 100 °C to 190 °C higher than those observed in experimental results [24]. However, this discrepancy is observed in only a few compositions in this work. Specially, only seven cases have a combined CaO + MgO content exceeding 55 mass%, and among these, only three have an MgO content greater than 15 mass%

The region within 35–40 mass% CaO corresponds for melting points between 1700 °C and 1550 °C, stepping slightly away for the typical characteristics of melting points for fayalitic slags in copper, lead, and zinc industries. Hence, the slags in these regions show composition derived from industrial steelmaking and synthetic slags with higher CaO/SiO_2 ratios. These types of slags are not normally called fayalitic slags due to their different chemical composition, which often include higher content of calcium, magnesium oxides and aluminosilicates. Therefore, the different types of slags are named differently depending on their origin, chemical composition, and physical properties [25]. The work by Piatak et al. [26] discusses the differences between slags produced during the recovery of nonferrous metals from natural ores (nonferrous slags) and ferrous slags, which are formed during recovery of iron from ores and iron-containing scrap. The study mentioned that the composition of ferrous slags are dominated by Ca and Si, with significant Fe content, while slags from nonferrous metallurgy are primarily composed of Fe and Si with lesser amounts of Al and Ca.

The fayalitic slags compositions revealed low and moderate melting temperatures. In the region near the fayalitic composition on the heat map, it is possible to observe that slight changes in the slag composition (mainly through CaO and SiO_2) can result in melting variations of up to approximately 400 °C.

According to a regression of the data [Eq. (10) and Table 3] it is observed that an increase in CaO content causes a greater effect on the increase of the melting temperature, followed by the same tendency for SiO_2 and FeO, however, less pronounced (see Fig. 3). The linear term for Al_2O_3 was omited from the model, as it was observed to exert a disturbing influence on the predictions and resulting in a lower R^2 during parameter optimization.

$$T_{\text{melting, model}} = \left(\begin{array}{c} a \cdot C_{\text{FeO}} + b \cdot C_{\text{SiO}_2} + c \cdot C_{\text{CaO}} + e \cdot C_{\text{MgO}} + f \cdot C_{\text{Fe}_2\text{O}_3} \\ + g \cdot C_{\text{FeO}} \cdot C_{\text{SiO}_2} + h \cdot C_{\text{FeO}} \cdot C_{\text{CaO}} + i \cdot C_{\text{SiO}_2} \cdot C_{\text{CaO}} \\ + j \cdot C_{\text{SiO}_2} \cdot C_{\text{MgO}} + k \cdot C_{\text{SiO}_2} \cdot C_{\text{Fe}_2\text{O}_3} + l \cdot C_{\text{CaO}} \cdot C_{\text{Al}_2\text{O}_3} \\ + m \cdot C_{\text{CaO}} \cdot C_{\text{MgO}} + n \cdot C_{\text{CaO}} \cdot C_{\text{Fe}_2\text{O}_3} + o \cdot C_{\text{Al}_2\text{O}_3} \cdot C_{MgO} \end{array} \right)^2 \quad (10)$$

Energy of Fusion

As shown in Fig. 4, to achieve a liquid state in fayalitic slags, a minimum of between 0.45 and 0.55 kWh/kg will be required. The higher the silica content, the higher the melting temperature and, therefore, the more energy will be required. If we take

Table 3 Regression coefficients to estimate the melting point and delta enthalpy of fusion of fayalitic slags

Term	Element (mass%)	Coefficients for melting temperature	Coefficients for ΔH_{fusion}
a	FeO	0.3955	0.007064
b	SiO_2	0.7382	0.013496
c	CaO	0.7967	0.013627
d	Al_2O_3	0.0	0.002526
e	MgO	1.5480	0.028230
f	Fe_2O_3	0.3097	0.007387
g	FeO*SiO_2	− 0.00703	− 0.00011
h	FeO*CaO	− 0.00708	− 9.3E−05
i	SiO_2*CaO	− 0.0078	− 0.00014
j	SiO_2*MgO	− 0.05128	− 0.00085
k	SiO_2*Fe_2O_3	− 0.0042	− 0.00011
l	CaO*Al_2O_3	− 0.00556	− 0.00011
m	CaO*MgO	− 0.01906	− 0.00026
n	CaO*Fe_2O_3	− 0.00256	0.0
o	Al2O3*MgO	0.03227	0.000632
p	Al2O3*Fe_2O3	0.0	0.000111
Evaluation		R^2 (predicted) = 99.93%	R^2 (predicted) = 99.93%

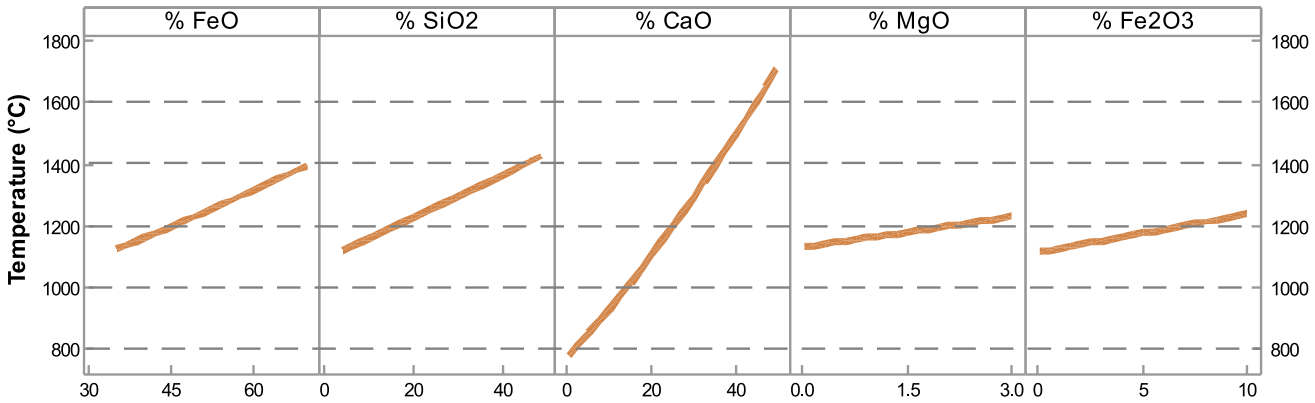

Fig. 3 Main effect plot for melting temperatures in Fayalitic slags

the isoenergic curve at 0.5 kWh/kg as a reference, we can see in Fig. 4b that adding up to 3 mass% MgO, 9 mass% Al_2O_3 or increasing the Fe^{3+} content to 10 mass% does not significantly alter the melting energy. It is the combination of these elements that increase the area where the energy required for slag melting is less than 0.5 kWh/kg. Table 3 presents the coefficients for the regression that allows us to estimate the fusion enthalpies of the green area in Fig. 4 through Eq. (11).

The regression analysis shows exactly the same behaviour as the melting temperature (see Fig. 3), and thus the remarks described for the melting temperatures also apply to the fusion enthalpies. The enthalpy variation or fusion energy (ΔH_{fusion}) can be used to estimate the energy requirements of a process, knowing that the minimum energy required in the process will be the ideal fusion energy divided by the furnace efficiency.

$$\Delta H_{fusion} = \left(\begin{array}{c} a \cdot C_{FeO} + b \cdot C_{SiO_2} + c \cdot C_{CaO} + d \cdot C_{Al_2O_3} + e \cdot C_{MgO} + f \cdot C_{Fe_2O_3} \\ +g \cdot C_{FeO} \cdot C_{SiO_2} + h \cdot C_{FeO} \cdot C_{CaO} + i \cdot C_{SiO_2} \cdot C_{CaO} \\ +j \cdot C_{SiO_2} \cdot C_{MgO} + k \cdot C_{SiO_2} \cdot C_{Fe_2O_3} + l \cdot C_{CaO} \cdot C_{Al_2O_3} \\ +m \cdot C_{CaO} \cdot C_{MgO} + o \cdot C_{Al_2O_3} \cdot C_{MgO} + p \cdot C_{Al_2O_3} \cdot C_{Fe_2O_3} \end{array} \right)^2 \quad (11)$$

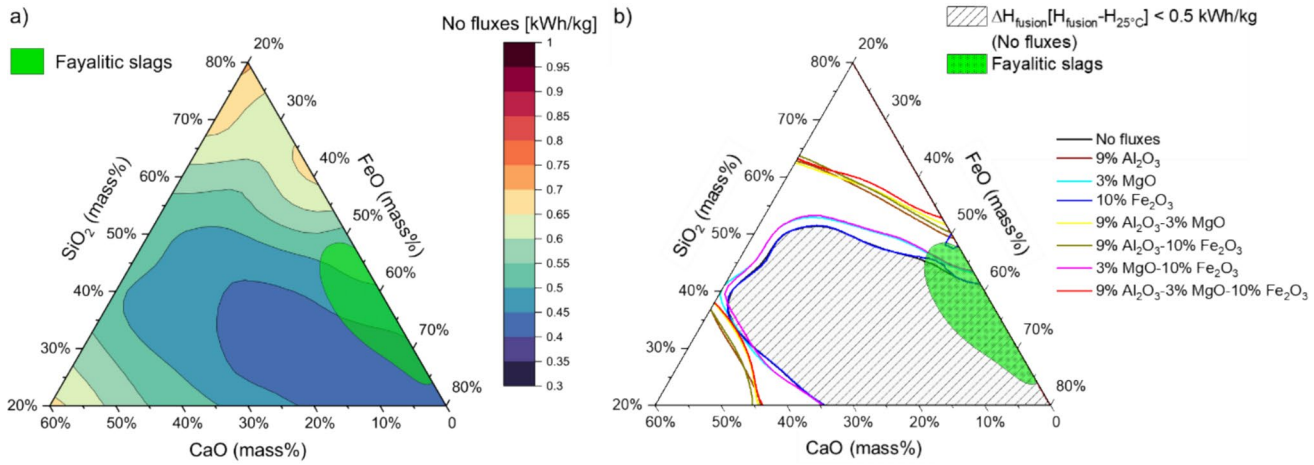

Fig. 4 Delta enthalpy of fusion: **a** primary compounds CaO–FeO–SiO_2; and **b** primary and secondary compounds (MgO, Fe_2O_3, and Al_2O_3) at 1200 °C. The green area in both graphs represents the majority composition of industrial fayalitic slags in Part I

According to some sources, melting processes in electric arc furnaces or some combustion furnaces have efficiencies of around 70 % and 60 %, respectively [27, 28]. Equation (12) can be used in combination with the information of the graph to estimate the energy requirement to melt fayalitic slags.

$$E_{\text{furnace}} = \frac{\Delta H_{\text{fusion}}}{\eta_{\text{f}}} \tag{12}$$

where E_{furnace} is the energy needed in kWh/kg of slag, ΔH_{fusion} is the variation of enthalpy between 25 °C and the melting temperature, and η_{f} is the thermal efficiency of the furnace utilized.

Viscosity

The ternary diagram in Fig. 5a shows the viscosity calculations for the primary compounds and Fig. 5b shows the same with the addition of secondary compounds at 1200 °C. This temperature was selected since it aligns to the typical range for fayalitic slags, supported by its consistency within the calculations of melting temperature shown in Chapter 3.1, and ensures comparability. The colored isoviscosity lines in Fig. 5b within the diagram represent different regions with specific flux additions according to the legend. At given fluxes addition, this hatched area expands or contracts, indicating an increase or decrease of this viscosity area—equal or lower than 1 Pa·s.

This region with viscosities below 1 Pa·s was chosen since practical studies have already demonstrated that this

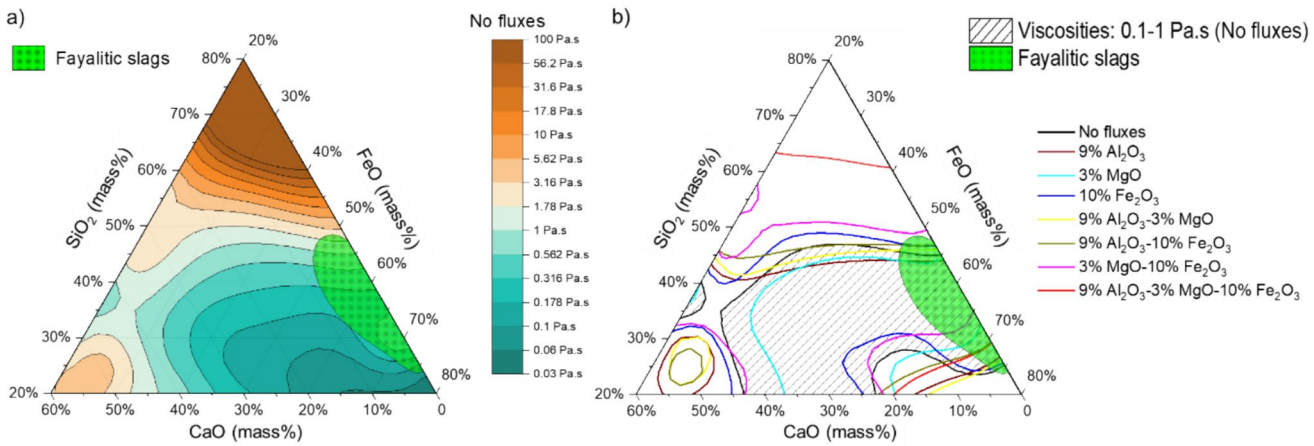

Fig. 5 Slag viscosity: **a** primary compounds CaO–FeO–SiO_2; and **b** primary and secondary compounds (MgO, Fe_2O_3, and Al_2O_3) at 1200 °C. The green area in both graphs represents the majority composition of industrial fayalitic slags in Part I

range is mostly found for CaO–Fe_xO_y–SiO_2 slags systems [29, 30]. Fayalitic slags have low-moderate viscosities (0.1–1 Pa·s), only reaching higher values than 3 Pa·s with a lower FeO/SiO_2 ratio content. These results are consistent with reported studies [29, 31, 32].

The green area in both charts indicates the region of the fayalitic slags encompassing the compositions studied from Part I. For these slags, viscosities from 0.075 to roughly 3 Pa·s [33] are observed, conferring a consistent viscosity characteristic mostly dependent of SiO_2 in molten FeO–SiO_2 systems [34]. For the fayalitic slags area, the color gradient transitions smoothly from turquoise at the lowest viscosity points to beige, where the highest viscosities were calculated for the studied fayalitic slags. According to the calculations, higher amounts of FeO are associated with lower viscosities, suggesting that increased iron oxide content reduced the slag's resistance to flow. The effectiveness of iron oxides in lowering the viscosity in such a melt system has already been noted, having a higher impact than CaO additions [35]. This can indeed be observed in Fig. 5b, where the addition of 10 mass% of hematite increases the area of the viscosity below 1 Pa·s (hatched area). This phenomenon can also be observed with additional fluxes, such as 3 mass% MgO and 9 mass% Al_2O_3. However, these two slagging components, once added separately (light blue and bordeaux lines), shrink this hatched area with viscosities ≤ 1 Pa·s. Hence, the shrinkage of this viscous area can be understood as a drawback in the composition range and similarly, in a narrow liquidus temperature zone. As a practical consequence, studies have shown that the unappropriated control of this area increases copper losses in fayalitic slags with high viscosity [29, 36]. For slags with a non-fayalite composition, where the impact of oxygen pressure on viscosity is negligible, the viscosity reaches its highest values in the lime and silica axis, where the basicity is unbalanced. In contrast, for melts with specific silica content, an increase in oxygen partial pressure significantly raises viscosity, due to further oxidation of iron oxides. As per the definition, the slag viscosity is inversely proportional to the settling velocity. In this context, understanding and controlling the composition, particularly FeO and SiO_2, is critical to manage viscosity and consequently reducing copper losses in slags [37, 38]. On the red isoviscosity line, the viscosities for compositions without fluxes that have the highest values (> 10 Pa·s) can be reduced with the addition of the fluxes shown, specifically Al, Mg, and Fe oxides, which can be advantageous when dealing with changes in compositions under different smelting conditions.

Equation (13) and Table 4 present the regression model and coefficients, respectively, for estimating the viscosity of Fayalitic slags (green area in Fig. 5).

$$\eta_s = \begin{pmatrix} -a \cdot C_{FeO} - b \cdot C_{SiO_2} \\ -c \cdot C_{CaO} - d \cdot C_{Al_2O_3} \\ -e \cdot C_{MgO} - f \cdot C_{Fe_2O_3} \\ +g \cdot T \end{pmatrix}^{-3.05507} \quad (13)$$

The analysis of the regression in Fig. 6 shows that SiO_2 is the main responsible for an exponential increase of the viscosity. Regarding FeO, this element will decrease the viscosity of the system. However, an excess will increase the activity of FeO, and once the iron activity increases, the system will react to produce a mixture of solid Fe_3O_4 and metallic iron. This solid presence will tend to modify the system's viscosity. Al_2O_3 and Fe_2O_3 exhibit an amphoteric character, acting as a network modifier or former, depending on the quantity present in the mix. For the remaining basic fluxes, such as CaO and MgO, substituting SiO_2 tends to reduce viscosity. However, if an excess of these substitutes influences FeO, it could increase the system's melting temperature. If this occurs at 1200 °C, the viscosity may increase. Therefore, maintaining viscosity control is a delicate balance between stabilizing FeO with silica and preventing silica excess, achieved through the use of basic fluxes like CaO and MgO, which ensure a basicity that results in low viscosities and low melting temperatures.

Density

Density (ρ) values in slags are crucial for understanding the behaviour and performance during metallurgical processes, playing a role in the settlement of metals (Stokes' law) [30]. Generally, the density of a slag is influenced by several factors, including temperature, composition, viscosity, and volume. As temperature increases, the density of most slags

Table 4 Regression coefficients to estimate the viscosity and the density of fayalitic slag

Term	Element (mass%)	Coefficients for viscosity	Coefficients for density
a	FeO	0.017458	0.01156
b	SiO_2	0.009957	0.07121
c	CaO	0.011718	0.00370
d	Al_2O_3	0.018062	0.05199
e	MgO	0.013886	0.01160
f	Fe_2O_3	0.014428	0.01909
g	Temperature (°C)	− 0.000260	− 0.004020
Evaluation		R^2 (predicted) = 99.94%	R^2 (predicted) = 97.70%

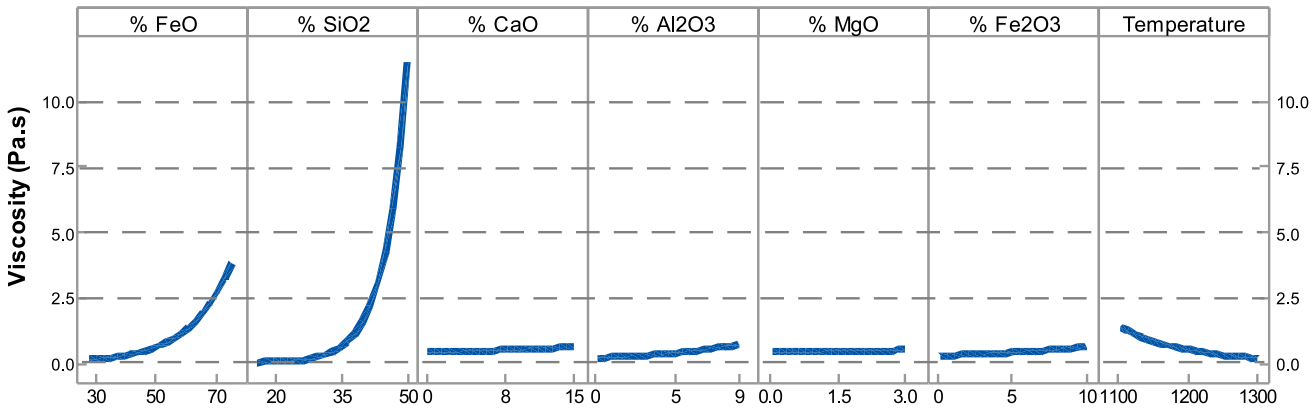

Fig. 6 Main effect plot for viscosity in fayalitic slags

tends to decrease due to thermal expansion; however, this relationship can vary based on the specific composition of the slag. In fayalitic slags, SiO_2 and various fluxing agents such as CaO or Al_2O_3 significantly affect the density by the proportions of these components. For instance, higher concentrations of metal oxides typically lead to an increase in density. Additionally, viscosity plays a critical role; as viscosity also changes with temperature and composition, it can affect how effectively metals are extracted from the slag phase. According to the method by Shu and Chou [12], the volume of the system and Gibbs energy play a significant role, which highlights the importance of thermochemical properties.

In Fig. 7, density is plotted against each compound and temperature independently. The results show that FeO content has a significant impact on density, followed by SiO_2. While the increase in temperature from 1100 to 1300 °C resulted in only a minor effect on density—indicating a decrease—this observation aligns with standard literature on thermal expansion [39]. As the temperature rises, molecules gain higher kinetic energy and move vigorously, increasing the distance between them. However, this range of 200 °C appears insufficient to cause a significant change in the behaviour of the compounds.

Equation (14) and Table 4 depict the equation and the coefficients to calculate the density of the fayalitic slags in the green are of Fig. 8a as a function of the system compounds composition.

$$\rho = \exp\left(a \cdot C_{FeO} + b \cdot C_{SiO_2} + c \cdot C_{CaO} + d \cdot C_{Al_2O_3} + e \cdot C_{MgO} + f \cdot C_{Fe_2O_3} + g \cdot T\right) \quad (14)$$

In Fig. 8a, the variation in slag density, ranging from 2.4 to 4 g·cm^{-3}, is represented in a ternary diagram of primary compounds (FeO, SiO_2, and CaO) at 1200 °C. This temperature was chosen because it represents an average condition where no significant changes in density occur. Again, the green area on the diagram indicates the composition range of fayalitic slag that is most commonly reported in industry (as discussed in Part I). Within this area, the density can take on seven different values, ranging from 2.9 to 3.5 g·cm^{-3}, depending on the specific composition. This demonstrates

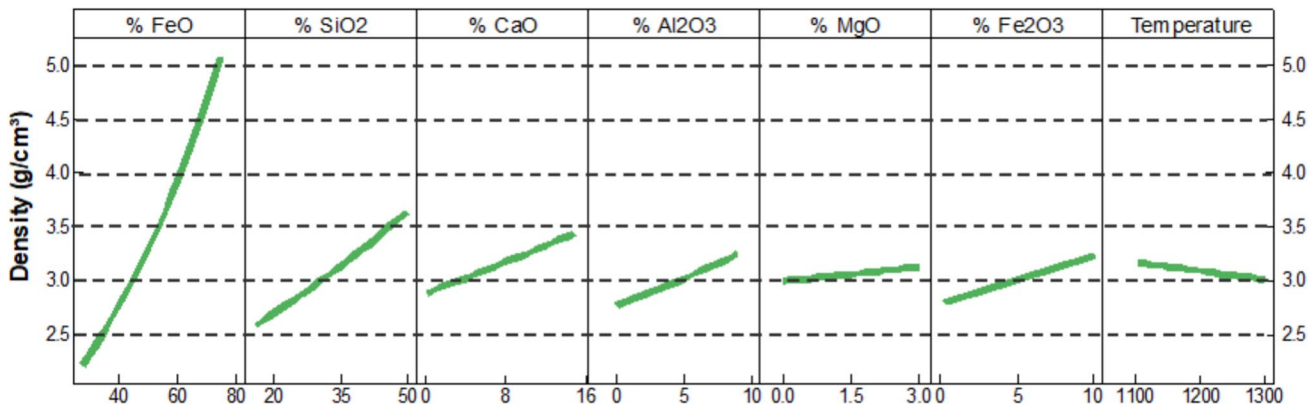

Fig. 7 Main effect plot for density in Fayalitic slags

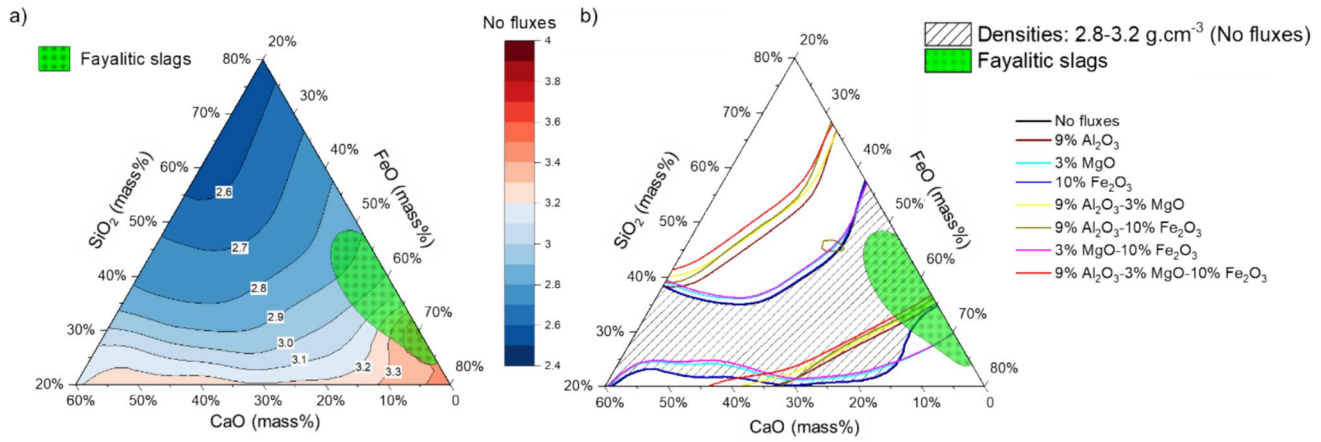

Fig. 8 Slag density: **a** primary compounds CaO–FeO–SiO_2; and **b** primary and secondary compounds (MgO, Fe_2O_3, and Al_2O_3) at 1200 °C. The green area in both graphs represents the majority composition of industrial fayalitic slags in Part I

that FeO and SiO_2 have a substantial influence on this property; specifically, as the FeO content increases, the density of the slag also increases.

When secondary compounds such as Al_2O_3, MgO, and Fe_2O_3 are incorporated into the ternary system, the density range between 2.8 and 3.2 g·cm^{-3} at 1200 °C is altered by the addition of each flux, as shown in Fig. 8b. A significant change occurs when 9 mass% Al_2O_3 is added to the system, regardless of the content of the other two fluxes, MgO and Fe_2O_3. The four areas representing the additions of Al_2O_3—colored red, yellow, dark yellow, and brown—are closely positioned but shifted toward lower FeO compositions. This shift expands the density area of 2.8–3.2 g·cm^{-3} from approximately 35 mass% to 65 mass% FeO, compared to its original range of about 45 mass% to 65 mass% FeO. In contrast, when MgO and Fe_2O_3 are added to this fayalitic slag without any Al_2O_3 addition, the resulting areas are nearly congruent with the lines representing the area without any fluxes (light blue, dark blue, and pink), indicating their minimal impact on density.

The density of fayalite mineral is 4.6 g·cm^{-3}; however, the addition of CaO results in a decrease in this value. According to Shiraishi et al. [34], different models predicted densities ranging from 3.5 to 5 g·cm^{-3} for compositions with up to 40 mol% SiO_2, although these predictions were based solely on binary systems containing FeO at 1400 °C. This suggests that the addition of CaO and other fluxes tends to lower the density values. At 1250 °C, Zhang et al. [40] reported that adding up to 10 mass% CaO to a system consisting of Fe-, Si-, and Ca-oxides decreases the density by approximately 0.3 g·cm^{-3}, resulting in a density of around 3.2 g·cm^{-3}. Conversely, the addition of Fe_3O_4 increases the density to about 3.5 g·cm^{-3}, though this effect is less pronounced. Most reports primarily evaluate the density of fayalite slags after granulation, meaning that the values correspond mainly to solid fractions that have been quenched. The average density reported in these studies was approximately 3.0 g·cm^{-3}; however, each report utilized different slag systems with varying compound compositions [41–49].

Distribution Coefficients of Metals Between Phases

Figure 9 illustrates the distribution coefficients of various metals between the slag and metal phases at a fixed temperature of 1200 °C, based on the normalized composition of fayalitic slags and FactSage™ calculations (see Chapter 2.2). The x-axis represents the system's oxygen partial pressure on a logarithmic scale, ranging from -23 to -10. The left *y*-axis indicates the distribution coefficient on a logarithmic scale (slag/metal ratio), and the right *y*-axis shows the carbon excess added to the system corresponded to the partial pressure depicted on the *x*-axis.

Distribution coefficients shed light on the nature and behavior of slags, and are also useful for understanding how to mobilize and separate different species present in the mineral phase. It is important to understand that slag fulfils several roles in pyrometallurgy, such as protecting the metallic phase from oxidation, improving the separation between a gangue (non-metallic inclusions) and a metal, and retaining as many impurities as possible to enhance metal quality and purity [19, 50].

Sasabe et al. [20, 52, 53] showed that amphoteric species like Fe increase exponentially the partial pressure of the system. A clear view of this is provided in Fig. 10, where a slag containing iron has an equilibrium partial pressure between 1×10^{-8} and 1×10^{-6} atm, which plays a key role in the immobilization of other elements [19]. Considering Fig. 9, fayalitic slag without the presence of a reductant, i.e., carbon, it will tend to keep all the

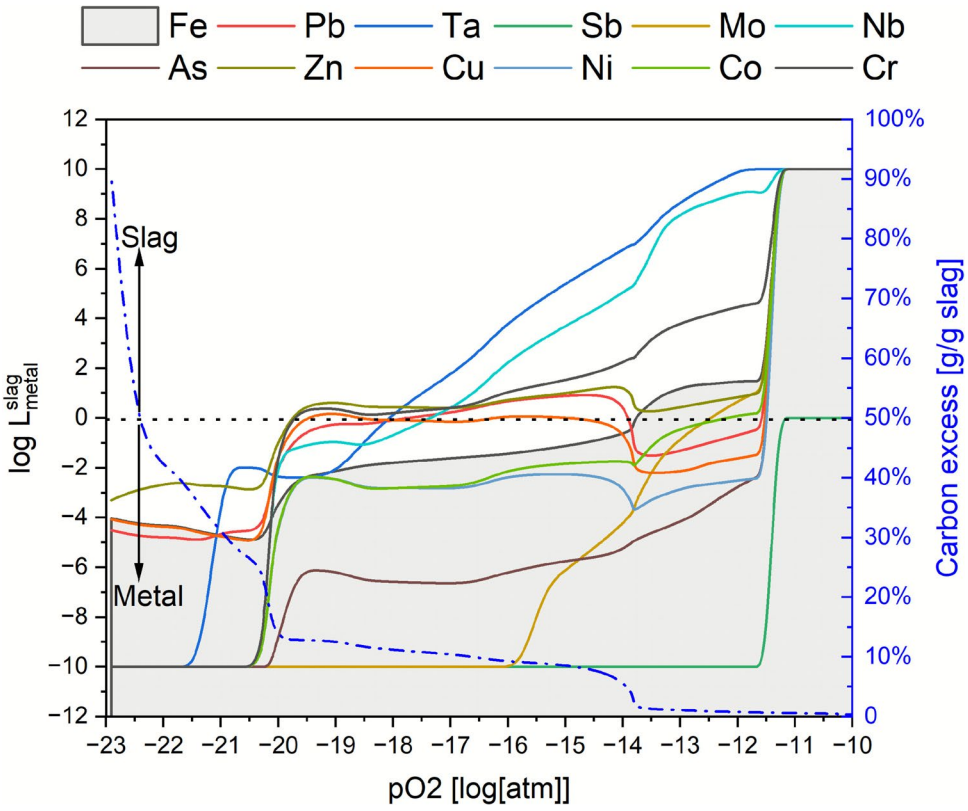

Fig. 9 Distribution coefficients of slag and metal phase for selected elements as a function of oxygen partial pressure, with excess carbon percentage shown on the right *y*-axis

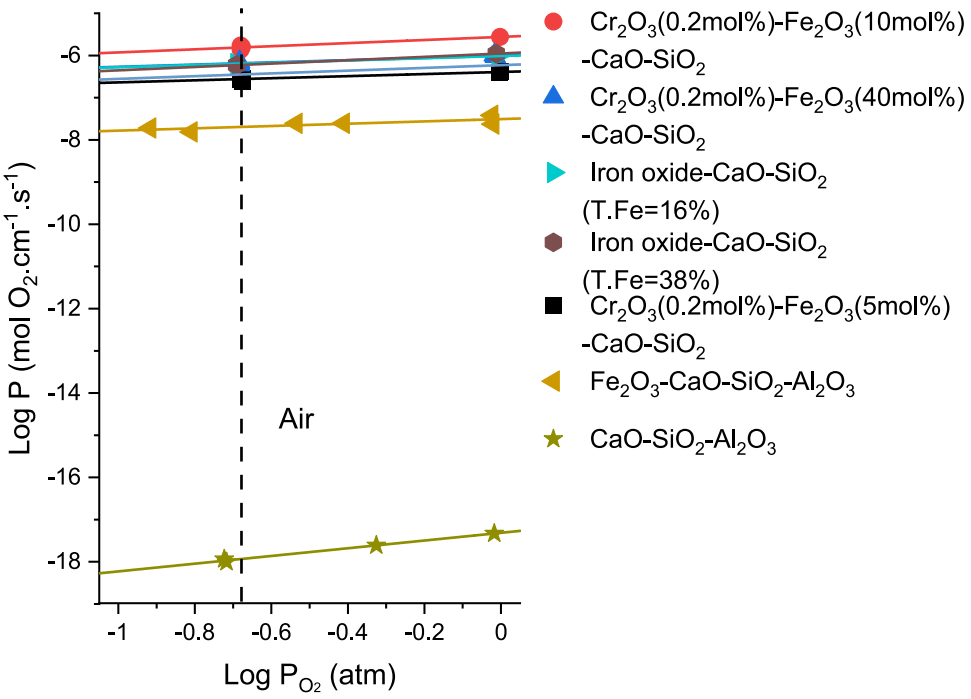

Fig. 10 Relationship between oxygen permeability (*P*) in an slag and a variable external oxygen partial pressure for several slag chemistries. Digitalized, adapted and reprinted by Lucas [51] from Sasabe et al. [20]

elements in the slag phase (partial pressures larger than 1×10^{-12} atm).

The gray area in Fig. 9 corresponds to the behavior of iron. When an excess of carbon starts promoting the reduction of iron, the partial pressure of the system will start decreasing. By removing this amphoteric specie (Fe) from the slag phase, the rest of the elements, more noble, will automatically increase their chemical activity. Thus, the

removal by fuming or in the form of metal becomes thermodynamically possible.

When the pO_2 of the system reaches 1×10^{-14} atm, the fraction of iron in the metal phase will overcome the fraction in the slag. This is equivalent to nearly 5 mass% of excess carbon. Once the pO_2 of the system continues to drop until it reaches 1×10^{-23}, more iron will be concentrated in the metal phase ($L \sim -4$). In addition, the excess of carbon equivalent will increase, but will not have a significant effect on the distribution coefficient. In other words, iron can be stabilized in the slag phase by controlling the amount of carbon in the process.

Pb, Zn, Cu, and Cr therefore form a group of similar behaviour, where, in a range from 1×10^{-14} to 1×10^{-20}, the metals present a constant L close to 0, meaning that both fractions, slag and metal, contain the same content. However, when the carbon excess suddenly increases to 25 mass%, the coefficient decreases, indicating that the metals have a higher concentration in the metal phase.

This distribution equilibrium can be noted in a wide range of oxygen partial pressure (1×10^{-14} to 1×10^{-20} atm). An example of the onset of iron reduction in a fayalitic slag system can be observed when molybdenum becomes more dissolved in the metal phase, the distribution line gets a more linear shape at around $\log pO_2 = 1 \times 10^{-13}$ atm, after which the concentrations of Cu and Pb in the slag increase, reaching nearly a phase distribution equilibrium. At partial pressures near 1×10^{-14} atm, the activity of metals like Pb, Zn, Cu, and Cr in the slag decreases, resulting in a reduction process, but the concentration of Fe in the slag is still higher. At moderate partial pressures, spinel (mostly magnetite) precipitation is expected to be problematic. During smelting under atmospheric conditions, FeO would oxidise in the liquid slag into magnetite, increasing slag viscosity and liquidus temperature at typical industrial temperatures of 1250–1300 °C, hence potentially freezing the melting. To counter this, a layer of coal coke is applied to the slag granules, as in industrial processes, creating a slightly reducing furnace atmosphere [54, 55]. This stabilization helps to immobilize or control the distribution of other accompanying metals by reducing their mobility between phases, so they can be selectively diluted into a targeted phase.

The graph also depicts the slag/metal distribution behavior for elements with higher oxygen affinity, such as Ta and Nb. Their reduction occurs at low oxygen partial pressures with a carbon excess greater than 10 mass%. This exemplifies that few metals, like Ta, are trapped in fayalitic slags, where the oxygen partial pressure is low (1×10^{-12} atm), depending primarily on the iron oxide content in the slag phase. Tantalum and Niobium, which behave similarly, will only have a content in the metal phase bigger than the slag phase in pO_2 1×10^{-18} atm and $1 \times 10^{-17.5}$ atm, respectively, which equals to an excess of carbon ~ 12 mass%, therefore to reduce Tantalum, more carbon has to be added, but the iron will have been reduced previously. In this situation, Ta and Nb are nearly all reduced already. Ni, Co, Mo, Sb, and As form a third group, where the coefficient distribution falls under zero at $\log pO_2 = 1 \times 10^{-12}$ atm, which requires nearly zero carbon excess for a reduction.

From a thermochemical perspective, reducing metals in low concentrations in fayalitic slag is possible. Nevertheless, an excess of carbon equal in mass to the slag to be treated will be required to make this happen theoretically. In real life, this is illogical.

The presence of iron creates conditions, such as high partial pressures, that allow fayalitic slags to melt at low temperature below 1200 °C. In nonferreous metallurgy, iron is often an undesired element in the metal phase, so it has been kept in the slag. However, this also causes a wide range of the other elements to be trapped in the slag at varying amounts. Some of these elements are valuable, like tantalum and niobium, while others are harmful, like lead, zinc, arsenic, antimony and chromium [6, 26, 56–59].

Limitations and Additional Work

While the thermodynamic models in this study assume equilibrium conditions, real-world industrial processes often deviate due to kinetic factors, which cannot be fully predicted. Expected variations include incomplete fayalite decomposition during cooling (leading to amorphous matrices with residual phases), elevated viscosities from slow diffusion, or altered metal distributions (e.g., higher Cu/Pb retention in slag due to limited reaction time). These introduce limitations such as overestimated melting temperatures (100–190 °C in high-CaO/MgO systems) or underestimated reduction extents (activation energies 175–248 kJ/mol slowing reactions). Additional work can incorporate experimental kinetic studies, such as controlled cooling rate experiments or diffusion rate measurements, to validate and refine these predictions, as discussed in Part I [11] regarding disequilibrium conditions from varying cooling regimes.

The limitations are exemplified when comparing studies with our model. For validation against experimental data, a direct comparison was made with viscosity measurements from Ji et al. [29]. Taking a composition close to stoichiometric fayalite (~ 70 mass% FeO, 30 mass% SiO_2), our model predicts a viscosity of ~ 0.1 Pa·s at 1200 °C, whereas in the reported study at 1250 °C the viscosity is 0.08 Pa·s, which shows an error of 20% considering the temperature difference and minor compositional variations. Additionally, for melting point, a direct comparison was made with data from Bowen et al. [60]. For stoichiometric fayalite (~ 71 mass% FeO, 29 mass% SiO_2), our model predicts a liquidus temperature of ~ 1200 °C, which aligns closely with the experimental value of 1205 °C reported in that study, showing a

negligible error of ~ 0.4%. It is important to consider that typical measurements uncertainties of ± 10 to 20 °C in high-temperature slag systems are already expected. These quantitative agreements support the model's reliability for fayalitic slag systems.

Conclusion

Evaluating the thermodynamic and physical properties of fayalitic slags is essential to understand reasonable slag valorization, as it provides insights into the behaviour of target metals in different mineralogical phases, enabling efficient metal recovery and mineral enrichment, while also offering operational advantages. The reprocessing of fayalitic slags extends beyond evaluating individual physical or chemical parameters (e.g., post-process slags and elution methods), enhancing how adjusting slag properties can influence the mobilization of critical metals, including environmentally relevant elements, thereby supporting a circular economy. In this context, by varying the composition of fayalitic slag compounds, as unraveled in Part I, properties such as viscosity, density, melting temperature, and enthalpy of fusion were simulated and assessed to propose further modifications in practical smelting operations. Within the range of industrial fayalitic slags' composition, their properties have also assumed significant variations. In general, an increase in individual compounds' content increases the mentioned properties. However, some specific compounds have a more significant effect than others. Contrary to general belief, the CaO increase is more significant for the raising of melting temperature. The SiO_2 is more significant for the viscosity, and the FeO is more significant for the density. Furthermore, the addition of secondary compounds has also an important effect on each property, which emphasises the complexity of such systems.

The combined addition of fluxes optimizes the working zones for properties like melting point and viscosity in fayalitic slags, even when significant compositional changes occur throughout different processes, thereby enhancing targeted mineral enrichment.

Finally, this work brings four simple graphs and regression models as tools for those working with fayalitic slags, providing an overview of their properties and how these can be evaluated across a wide range of compositions and additives. It is expected that this could be utilized by metallurgists and other specialists working with fayalitic slags to obtain easily the properties such as energy needs, melting temperatures, viscosity, or density related to their manipulation. The equations offer a practical alternative to complex simulations, allowing industrial users to optimize slag properties in real-time for enhanced metal recovery and operational efficiency in fayalitic systems, though validated within the compositional ranges from Part I [11] and not suited for automatic real-time adjustments beyond those limits.

By breaking down complex thermodynamic simulations and the resulting equations describing key physical properties, this study contributes to sustainable metallurgy on supporting the circular economy through closing potential gaps in metal recovery from slags, minimizing environmental impacts such as reduced emissions and waste in smelting operations via optimized process efficiency.

Funding Open Access funding enabled and organized by Projekt DEAL. This research was funded by the German Research Foundation (DFG) within the scope of the priority program "Engineered Artificial Minerals (EnAM)—a geo-metallurgical tool to recycle critical elements from waste streams" (SPP2315).

Declarations

Conflict of interest The authors report there is no confict of interest to declare.

References

1. Alvear Flores GRF, Nikolic S, Mackey PJ (2014) ISASMELT™ for the recycling of e-scrap and copper in the U.S. case study example of a new compact recycling plant. JOM 66:823–832. https://doi.org/10.1007/s11837-014-0905-3
2. Banda W, Morgan N, Eksteen J (2002) The role of slag modifiers on the selective recovery of cobalt and copper from waste smelter slag. Miner Eng 15:899–907. https://doi.org/10.1016/S0892-6875(02)00090-0
3. Grimsey E (ed) (1992) Non-ferrous melt chemistry: the roles of slags and mattes. Springer, New York
4. Shi C, Meyer C, Behnood A (2008) Utilization of copper slag in cement and concrete. Resour Conserv Recycl 52:1115–1120. https://doi.org/10.1016/j.resconrec.2008.06.008
5. Schepper M, Verlé P, van Driessche I et al (2015) Use of secondary slags in completely recyclable concrete. J Mater Civ Eng. https://doi.org/10.1061/(ASCE)MT.1943-5533.0001133
6. Potysz A, van Hullebusch ED, Kierczak J et al (2015) Copper metallurgical slags—current knowledge and fate: a review. Crit Rev Environ Sci Technol 45:2424–2488. https://doi.org/10.1080/10643389.2015.1046769
7. GTT Technologies (2020) Slagatlas: HotVeGas 16:839

8. Zhao B, Jak E, Hayes PC (1999) The effect of Al2O3 on liquidus temperatures of fayalite slags. Metall Mater Trans B 30:597–605. https://doi.org/10.1007/s11663-999-0020-y
9. Geissdoerfer M, Savaget P, Bocken NM et al (2017) The circular—a new sustainability paradigm? J Clean Prod 143:757–768. https://doi.org/10.1016/j.jclepro.2016.12.048
10. Antony Jose S, Calhoun J, Renteria OB et al (2024) Promoting a circular economy in mining practices. Sustainability 16:11016. https://doi.org/10.3390/su162411016
11. Weiss J, Munchen D, Lucas H et al (2026) Fayalitic minerals and dlags (Part I): a survey on composition and potential for phases design. J Sustain Metall. https://doi.org/10.1007/s40831-025-01387-7
12. Shu QF, Chou K-C (2013) Calculation for density of molten slags using optical basicity. Ironmaking Steelmaking 40:571–577. https://doi.org/10.1179/1743281212Y.0000000083
13. Allibert M (2008) Slag atlas, 2nd edn. Repr. without change. Verl. Stahleisen, Düsseldorf
14. Toop G, Samis C (1962) Activities of ions in silicate melts. Trans Metall Soc AIME 224:878–887
15. Toop GW, Somis CS (1962) Some new ionic concepts of silicate slags. Can Metall Q 1:129–152. https://doi.org/10.1179/cmq.1962.1.2.129
16. Ottonello G, Moretti R, Marini L et al (2001) Oxidation state of iron in silicate glasses and melts: a thermochemical model. Chem Geol 174:157–179. https://doi.org/10.1016/S0009-2541(00)00314-4
17. Roscoe R (1952) The viscosity of suspensions of rigid spheres. Br J Appl Phys 3:267–269. https://doi.org/10.1088/0508-3443/3/8/306
18. Seetharaman S, Mukai K, Sichen D (2005) Viscosities of slags—an overview. Steel Res Int 76:267–278. https://doi.org/10.1002/srin.200506008
19. Krüger J (1999) Metalle–Speisen–Steine–Schlacken; Grundlegende Eigenschaften Und Reaktionen. Schlacken in der Metallurgie: Vorträge beim 35. Metallurgischen Seminar des Fachausschusses für Metallurgische Aus- und Weiterbildung der GDMB vom 17. bis 19. März 1999 in Aachen. GDMB-Informationsges, Clausthal-Zellerfeld, pp 9–38
20. Sasabe M, Asamura A (1984) Transport phenomenon of oxygen through molten slags. In: 1984 Second International Symposium on Metallurgical, pp 651–668
21. Mackwell SJ (1992) Oxidation kinetics of fayalite (Fe2SiO4). Phys Chem Miner 19:220–228. https://doi.org/10.1007/BF00202311
22. Alkan G, Mechnich P, Lucas H et al (2022) Assessment of metallurgical slags as solar heat absorber particles. Minerals 12:121. https://doi.org/10.3390/min12020121
23. Chen M, Avarmaa K, Taskinen P et al (2021) Handling trace elements in WEEE recycling through copper smelting-an experimental and thermodynamic study. Miner Eng 173:107189. https://doi.org/10.1016/j.mineng.2021.107189
24. Liao J, Qing G, Zhao B (2023) Phase equilibria studies in the CaO-MgO-Al2O3-SiO2 system with Al2O3/SiO2 weight ratio of 0.4. Metals 13:224. https://doi.org/10.3390/met13020224
25. Kirschen M, Hay T, Echterhof T (2021) Process improvements for direct reduced iron melting in the electric arc furnace with emphasis on slag operation. Processes 9:402. https://doi.org/10.3390/pr9020402
26. Piatak NM, Parsons MB, Seal RR (2015) Characteristics and environmental aspects of slag: a review. Appl Geochem 57:236–266. https://doi.org/10.1016/j.apgeochem.2014.04.009
27. Makarov AN, Okuneva VV, Pavlova YM (2020) Calculation and analysis of the arcs efficiency of small and large capacity arc steel-melting furnaces. IOP Conf Ser 791:12032. https://doi.org/10.1088/1757-899X/791/1/012032
28. Semenov S, Namy P, Kale A et al (2024) Numerical model of a top-blown rotary converter preheating and charge heating with an oxy-fuel burner. Open Res Eur 4:248. https://doi.org/10.12688/openreseurope.18594.2
29. Ji F-Z, Du S, Seetharaman S (1997) Experimental studies of the viscosities in the CaO-Fe n O-SiO2 slags. Metall Mater Trans B 28:827–834. https://doi.org/10.1007/s11663-997-0010-x
30. Kondratiev A, Jak E (2001) Modeling of viscosities of the partly crystallized slags in the Al_2O_3-CaO-"FeO"-SiO_2 system. Metall Mater Trans B 32:1027–1032. https://doi.org/10.1007/s11663-001-0091-x
31. Eguchi T, Nishioka N, Takebe H (2023) Additive effect of Al_2O_3, CaO, and MgO on the viscosity of FeO_x–SiO_2 slag melt (x = 1.0–1.5). J Sustain Metall 9:1487–1498. https://doi.org/10.1007/s40831-023-00741-x
32. Viswanathan NN, Ji F-Z, Du S et al (2001) Viscosity measurements on some fayalite slags. ISIJ Int 41:722–727. https://doi.org/10.2355/isijinternational.41.722
33. Xiao W, Yao S, Zhou S et al (2022) Evolution of the structure and viscosity of copper slag during metallization-reduction. J Alloys Compd 903:163751. https://doi.org/10.1016/j.jallcom.2022.163751
34. Shiraishi Y, Ikeda K, Tamura A et al (1978) On the viscosity and density of the molten FeO–SiO_2 system. Trans JIM 19:264–274. https://doi.org/10.2320/matertrans1960.19.264
35. Zhang L, Jahanshahi S (1998) Review and modeling of viscosity of silicate melts: Part I. Viscosity of binary and ternary silicates containing CaO, MgO, and MnO. Metall Mater Trans B 29:177–186. https://doi.org/10.1007/s11663-998-0020-3
36. Poggi D, Minto R, Davenport WG (1969) Mechanisms of metal entrapment in slags. JOM 21:40–45. https://doi.org/10.1007/BF03378796
37. Friedrich B, Kalisch M, Friedmann D et al (2018) The submerged arc furnace (SAF): state-of-the-art metal recovery from nonferrous slags. J Sustain Metall 4:77–94. https://doi.org/10.1007/s40831-017-0153-1
38. Kaya F, Khadhraoui S, Derin B (2018) A modelling investigation on the viscosity of fayalite slags by FactSage. In: Conference: 19th International Metallurgy and Materials Congress
39. Bottinga Y, Weill D, Richet P (1982) Density calculations for silicate liquids. I. Revised method for aluminosilicate compositions. Geochim Cosmochim Acta 46:909–919. https://doi.org/10.1016/0016-7037(82)90047-3
40. Zhang H, Fu L, Qi J et al (2019) Physicochemical properties of the molten iron-rich slags related to the copper recovery. Metall Mater Trans B 50:1852–1861. https://doi.org/10.1007/s11663-019-01611-2
41. Addis A, Angelini I, Nimis P et al (2016) Late bronze age copper smelting slags from Luserna (Trentino, Italy): interpretation of the metallurgical process. Archaeometry 58:96–114. https://doi.org/10.1111/arcm.12160
42. Adediran A, Yliniemi J, Illikainen M (2021) Mineralogy and glass content of Fe-rich fayalite slag size fractions and their effect on alkali activation and leaching of heavy metals. Int J Ceram Engine Sci 3:287–300. https://doi.org/10.1002/ces2.10107
43. Adediran A, Yliniemi J, Lemougna PN et al (2023) Recycling high volume Fe-rich fayalite slag in blended alkali-activated materials: effect of ladle and blast furnace slags on the fresh and hardened state properties. J Build Eng 63:105436. https://doi.org/10.1016/j.jobe.2022.105436
44. Alp I, Deveci H, Süngün H (2008) Utilization of flotation wastes of copper slag as raw material in cement production. J Hazard Mater 159:390–395. https://doi.org/10.1016/j.jhazmat.2008.02.056
45. Ambily PS, Umarani C, Ravisankar K et al (2015) Studies on ultra high performance concrete incorporating copper slag as

fine aggregate. Constr Build Mater 77:233–240. https://doi.org/10.1016/j.conbuildmat.2014.12.092
46. Gorai B, Jana RK, Premchand (2003) Characteristics and utilisation of copper slag—a review. Resour Conserv Recycl 39:299–313. https://doi.org/10.1016/S0921-3449(02)00171-4
47. Lim T-T, Chu J (2006) Assessment of the use of spent copper slag for land reclamation. Waste Manag Res 24:67–73. https://doi.org/10.1177/0734242X06061769
48. Madheswaran CK, Ambily PS, Dattatreya JK et al (2014) Studies on use of copper slag as replacement material for river sand in building constructions. J Inst Eng India Ser A 95:169–177. https://doi.org/10.1007/s40030-014-0084-9
49. Murari K, Siddique R, Jain KK (2015) Use of waste copper slag, a sustainable material. J Mater Cycles Waste Manag 17:13–26. https://doi.org/10.1007/s10163-014-0254-x
50. Mousa H, Agterof W, Mellema J (2001) Theoretical and experimental investigation of the coalescence efficiency of droplets in simple shear flow. In: Koutsoukos PG (ed) Trends in Colloid and Interface Science XV: 14th Conference of the European Colloid and Interface Society, September 2000 in Patras, Greece, vol 118. Springer, Berlin, pp 208–215
51. Lucas HI Valorisation of municipal solid waste incineration bottom ash for use as construction material. Dissertation, Shaker Verlag; Rheinisch-Westfälische Technische Hochschule Aachen
52. Sasabe M, Goto KS (1974) Permeability, diffusivity, and solubility of oxygen gas in liquid slag. Metall Trans 5:2225–2233. https://doi.org/10.1007/BF02643937
53. Sasabe M, Jibiki M (1983) Permeability of oxygen through molten slag containing iron oxide. Can Metall Q 22:29–36. https://doi.org/10.1179/cmq.1983.22.1.29
54. Kongoli F, McBow I, Yazawa A (2011) Phase relations of ferrous calcium silicate slag and its possible application in the industrial practice. High Temp Mater Process. https://doi.org/10.1515/htmp.2011.072
55. Zhao B, Hayes P, Jak E (2013) Effects of CaO, Al2O3 and MgO on liquidus temperatures of copper smelting and converting slags under controlled oxygen partial pressures. J Min Metall B 49:153–159. https://doi.org/10.2298/JMMB120812009Z
56. European Commission (2020) Critical raw materials resilience: charting a path towards greater security and sustainability. Publications Office of the European Union
57. European Commission, Directorate-General for Internal Market, Industry, Entrepreneurship, SMEs et al (2023) Study on the critical raw materials for the EU 2023—Final report. Publications Office of the European Union
58. Kero Andertun J, Samuelsson C, Peltola P et al (2022) Characterisation and leaching behaviour of granulated iron silicate slag constituents. Can Metall Q 61:14–23. https://doi.org/10.1080/00084433.2021.2016345
59. European Commission (2025) Directive-1999/31-EN-EUR-Lex. https://eur-lex.europa.eu/eli/dir/1999/31/oj. Accessed 22 Sept 2025
60. Bowen NL, Schairer JF, Posnjak E (1933) The system CaO-FeO-SiO_2. Am J Sci 5(153):26–258